

## The Use of a Tropism-Modified Measles Virus in Folate Receptor – Targeted Virotherapy of Ovarian Cancer

Kosei Hasegawa,<sup>1</sup> Takafumi Nakamura,<sup>1</sup> Mary Harvey,<sup>2</sup> Yasuhiro Ikeda,<sup>1</sup> Ann Oberg,<sup>3</sup> Mariangela Figini,<sup>5</sup> Silvana Canevari,<sup>5</sup> Lynn C. Hartmann,<sup>4</sup> and Kah-Whye Peng<sup>1</sup>

**Abstract Purpose:** Attenuated measles viruses are promising experimental anticancer agents currently being evaluated in a phase I dose escalation trial for ovarian cancer patients. Virus attachment, entry, and subsequent intercellular fusion between infected and uninfected neighboring cells are mediated via the two measles receptors (CD46 and SLAM). To minimize potential toxicity due to measles virus – associated immunosuppression and infection of nontarget tissues, we sought to develop an ovarian cancer exclusive fully retargeted measles virus.

**Experimental Design and Results:** Interactions of measles virus with its natural receptors were ablated, and a single-chain antibody (scFv) specific for  $\alpha$ -folate receptor (FR $\alpha$ ), a target overexpressed on 90% of nonmucinous ovarian cancer, was genetically engineered on the viral attachment protein (MV- $\alpha$ FR). Specificity of virus tropism was tested on tumor and normal cells. Biodistribution of measles virus infection was evaluated in measles-susceptible CD46 transgenic mice, whereas antitumor activity was monitored noninvasively by bioluminescence imaging in xenograft models. Tropism and fusogenic activity of MV- $\alpha$ FR was redirected exclusively to FR $\alpha$  without compromise to virus infectivity. In contrast to the parental virus, MV- $\alpha$ FR has no background infectivity on normal human cells. The antitumor activity of MV- $\alpha$ FR, as assessed by tumor volume reduction and overall survival increase, was equal to the parental virus in two models of human ovarian cancer (s.c. and i.p.).

**Conclusions:** A FR-exclusive ovarian cancer targeted oncolytic virus was generated and shown to be therapeutically effective, thus introducing a new modality for FR targeting and a candidate measles virus for clinical testing.

Live attenuated measles virus has promising oncolytic activity against a variety of tumor cells and xenografts (1, 2). Two recombinant measles viruses engineered for noninvasive monitoring of the pharmacokinetics of viral gene expression through the use of a soluble marker peptide (MV-CEA) or the human thyroïdal sodium iodide symporter (MV-NIS) are being tested in phase I clinical trials for patients with recurrent ovarian cancer, glioblastoma, and multiple myeloma (3–5). Measles virus uses its coat protein, hemagglutinin (H), to

attach to one of two viral receptors, CD46 or SLAM (signaling lymphocyte activation molecule), and the fusion (F) protein to mediate virus entry and subsequent virus spread by cell-to-cell fusion (6, 7). Thus, a unique feature of measles virus tumor cell killing is an extensive cytopathic effect of syncytial formation, which, in addition to viral replication, significantly increases bystander killing of neighboring cells by the agent (1, 8).

To minimize virus sequestration by non-target cells and collateral damage to normal tissues, the tropism and cytopathic activity of an oncolytic virus should ideally be restricted to tumor cells. The measles CD46 receptor, a regulator of complement activation, is ubiquitously expressed on all nucleated human cells, whereas SLAM is expressed on immune cells (7, 9). The characteristic immunosuppression associated with measles infection is thought to be due to interaction of measles H protein with CD46 and/or SLAM (10, 11). Hence, we recently engineered mutations in the H protein to ablate virus interactions with its native receptors and established a virus rescue system using a pseudoreceptor (His-6 tag) that allowed rescue and propagation of CD46/SLAM blind, fully retargeted measles viruses displaying scFv against CD38 (MV- $\alpha$ CD38) and the epidermal growth factor receptor (EGFR), MV- $\alpha$ EGFR (12).

Epithelial ovarian cancer is the leading cause of gynecologic cancer death in the United States, but neither MV- $\alpha$ CD38 nor MV- $\alpha$ EGFR is ideal for ovarian cancer therapy (13). EGFR is a nonspecific target as it is expressed on most epithelial cells,

**Authors' Affiliations:** <sup>1</sup>Molecular Medicine Program, <sup>2</sup>Toxicology Core, <sup>3</sup>Biostatistics, and <sup>4</sup>Medical Oncology, Mayo Clinic College of Medicine, Rochester, Minnesota; and <sup>5</sup>Department of Experimental Oncology, Unit of Molecular Therapies, Instituto Nazionale Tumori, Milan, Italy  
Received 4/21/06; revised 6/15/06; accepted 6/26/06.

**Grant support:** Minnesota Ovarian Cancer Alliance, Mayo Foundation, and Olivier S and Jennie R Donaldson Charitable Trust.

The costs of publication of this article were defrayed in part by the payment of page charges. This article must therefore be hereby marked *advertisement* in accordance with 18 U.S.C. Section 1734 solely to indicate this fact.

**Note:** Supplementary data for this article are available at Clinical Cancer Research Online (<http://clincancerres.aacrjournals.org/>).

Current address for T. Nakamura: Department of Molecular Genetics, Medical Institute of Bioregulation, Kyushu University, Fukuoka, Japan.

**Requests for reprints:** Kah-Whye Peng, Molecular Medicine Program, Mayo Clinic College of Medicine, 200 First Street SW, Rochester, MN 55905. Phone: 507-284-8357; Fax: 507-284-8388; E-mail: Peng.Kah@mayo.edu.

©2006 American Association for Cancer Research.  
doi:10.1158/1078-0432.CCR-06-0992

whereas CD38, a plasma cell marker, is not found on ovarian cancer cells. Among the membrane-associated targets, the  $\alpha$ -folate receptor (FR $\alpha$ ) is highly promising (14, 15). Elevated expression of FR $\alpha$  has been observed in various types of cancers, including ovarian, uterine, endometrial carcinoma, and pleural mesothelioma (14, 16–19). FR $\alpha$  expression in normal tissues is restricted to the apical surfaces of polarized epithelial cells where it is inaccessible to circulating cytotoxic drugs (14, 15, 17). Hence, there is much interest to use FR as target for tumor-specific killing using various types of anticancer therapeutics but none yet with a replicating oncolytic virus (14, 20).

In the current study, we generated a tropism modified measles virus displaying a FR $\alpha$ -specific scFv derived from MOv18, a monoclonal antibody that has been extensively tested in ovarian cancer clinical trials (21–23). The FR $\alpha$ -targeted measles virus can infect and destroy FR $\alpha$ -positive tumors efficiently and exclusively via the displayed scFv, warranting further investigation as a retargeted measles virus for clinical testing.

## Materials and Methods

**Cell culture.** Cell lines were purchased from the American Type Culture Collection (Manassas, VA) or have been described previously (12, 24–27). Peripheral blood lymphocytes from healthy volunteers were stimulated with 5  $\mu$ g/mL phytohemagglutinin for 6 days before use. A375-FR, ARH-77-FR, CHO-FR, and SKOV3ip.1-Fluc- $\beta$ hCG cells were generated by transduction of parental cells using VSV-G pseudotyped lentiviral vectors. To generate the lentivectors, 293T cells were cotransfected with gag-pol expression plasmid pCMV $\Delta$ 8.91, VSV.G envelope expression plasmid pMD-G, and vector plasmid pHR-SIN-dlNotI encoding cDNAs for expression of FR $\alpha$ , firefly luciferase (Fluc), or the  $\beta$  chain of human chorionic gonadotropin ( $\beta$ hCG; ref. 28). Supernatant was collected 48 hours later and frozen at  $-80^{\circ}\text{C}$ .

**Flow cytometry.** Cells were incubated for 30 minutes on ice with MOv18 (a mouse anti-FR $\alpha$  monoclonal antibody at 1:100 dilution), washed twice, and incubated for 30 minutes with 1:150 dilution of FITC-conjugated goat anti mouse IgG (Santa Cruz Biotechnology, Santa Cruz, CA). After washing, the cells were fixed and analyzed by flow cytometry using FACSscan with CellQuest software (Becton Dickinson, San Jose, CA).

**Generation of FR $\alpha$ -retargeted measles virus.** The cDNA for MOv18, an anti-FR $\alpha$  scFv (kindly provided by Dr. Y. Takeuchi, UCL, London), was PCR amplified as an *SfiI/NotI* fragment and inserted in-frame into pTNH6aa, a shuttle vector encoding measles H and containing alanine substitutions at residues 481 and 533 (Fig. 1A). The *PacI/SpeI* fragment was then inserted into p(+)-MV-eGFP. For rescue of FR $\alpha$ -retargeted virus, the Six-his Tagging and Retargeting system was used (12). Virus stocks were harvested after infection of Vero- $\alpha$ His cells at a multiplicity of infection of 0.02, and cell-associated viruses were harvested by freeze-thaw cycles. Virus stocks were titrated by 50% tissue culture infective dose (TCID<sub>50</sub>) assay on Vero- $\alpha$ His cells.

**Immunoblotting.** Viral samples ( $10^5$  TCID<sub>50</sub>; virus titer determined on Vero- $\alpha$ His cells) were directly mixed with an equal volume of SDS loading buffer [130 mmol/L Tris (pH 6.8), 20% glycerol, 10% SDS, 0.02% bromophenol blue, 100 mmol/L DTT]. These samples were denatured for 5 minutes at  $95^{\circ}\text{C}$ , fractionated on a 7.5% SDS-polyacrylamide gel, blotted to nitrocellulose membrane (Amersham, Piscataway, NJ), and immunoblotted with anti-measles N and H protein as described previously (12).

**Virus titration and infection.** To compare growth characteristics of the recombinant viruses, Vero- $\alpha$ His cells were infected with the viruses at a multiplicity of infection of 3.0 for 2 hours at  $37^{\circ}\text{C}$ . The inoculum was removed; the standard medium was replaced; and the cells were maintained at  $32^{\circ}\text{C}$ . At 12, 24, 36, 48, and 72 hours after infection, cells were scraped into 1 mL Opti-MEM (Life Technologies, Rockville, MD), and cell-associated viruses were released by two freeze-thaw cycles. Viral titers were determined by TCID<sub>50</sub> titration on Vero- $\alpha$ His cells. For virus infection, cells ( $10^5$  adherent cells or  $10^6$  suspension cells) were incubated with virus at a multiplicity of infection of 0.5 for 3 hours at  $37^{\circ}\text{C}$ . At 48 hours after infection, cells were photographed under fluorescence microscopy, and cell viability was determined by trypan blue exclusion assay.

**In vivo experiments and noninvasive monitoring of tumor burden.** All procedures involving animals were approved by and done according to guidelines of the Institutional Animal Care and Use Committee of Mayo Foundation. For *in vivo* targeting experiments,  $2 \times 10^6$  ARH-77 or ARH-77-FR cells were implanted s.c. in the right flank of irradiated severe combined immunodeficient mice (150 cGy). When the tumors reached 0.5 cm in diameter, two doses of  $2 \times 10^6$  TCID<sub>50</sub> MV-GFP, MV- $\alpha$ FR, or MV- $\alpha$ EGFR ( $n = 3$  per group) were injected i.v. at 2 days apart. Four days after the last injection, mice were euthanized, and tumors were examined under fluorescence microscopy. For virus biodistribution analysis, 7- to 9-week-old measles susceptible Ifnar-CD46Ge transgenic mice (29) were given 1 dose of  $2 \times 10^6$  TCID<sub>50</sub> MV-GFP or MV- $\alpha$ FR i.p. ( $n = 3$  per group). Mice were euthanized 48 hours later and analyzed as described previously (30). For the therapy experiments,  $2 \times 10^6$  SKOV3ip.1 cells were implanted s.c. in the right flank of female athymic mice (5–6 weeks of age; Taconic Laboratory, Germantown, NY). When the tumors reached 0.5 cm in diameter, mice received i.t. injections of MV-GFP ( $n = 10$  mice per group), MV- $\alpha$ FR ( $n = 10$ ) at  $5 \times 10^5$  TCID<sub>50</sub> in 100  $\mu$ L Opti-MEM, or vehicle (saline) control ( $n = 9$ ), every other day for a total four doses (total dose =  $2 \times 10^6$  TCID<sub>50</sub>). In the i.p. ovarian cancer model, SKOV3ip.1 cells stably expressing Fluc and  $\beta$ hCG were used to enable noninvasive monitoring of tumor burden during the course of virotherapy. Mice were implanted i.p. with  $2 \times 10^6$  SKOV3ip.1-Fluc- $\beta$ hCG cells. Six days later, mice were received six doses (given every other days) of MV-GFP ( $n = 10$ ), MV- $\alpha$ FR ( $n = 10$ ) at  $10^6$  TCID<sub>50</sub> in 500  $\mu$ L Opti-MEM, or saline ( $n = 9$ ) i.p. To monitor tumor burden, cohorts of five mice were bled for  $\beta$ hCG measurements and imaged using the IVIS 200 Bioluminescence Imaging System (Xenogen Corp., Alameda, CA). Plasma  $\beta$ hCG analysis was done by Mayo Clinic Central Clinical Laboratory. For imaging, mice were given i.p. injections of 150 mg/kg D-luciferin (Xenogen) 10 minutes before imaging. To quantitate tumor burden, whole abdominal bioluminescence signals were calculated from the imaging data using the Living Image software (Xenogen) according to manufacturer's protocol.

**Statistical analysis.** The differences in tumor burden (tumor volume, photon counts, and plasma  $\beta$ hCG) in each group were analyzed by two-way repeated measures ANOVA. Survival curves were represented using the Kaplan-Meier method. The log-rank test was used to examine the significance of differences in the survival between groups. We used GraphPad Prism (GraphPad Software, San Diego, CA) for the statistical calculations.  $P < 0.05$  was considered significant.

## Results

**Generation and characterization of FR $\alpha$ -retargeted measles virus.** The CD46/SLAM blind MV- $\alpha$ FR (Fig. 1A) was rescued and propagated via H6 peptide binding to its pseudoreceptor on Vero- $\alpha$ His cells as described previously (12). Correct incorporation of the scFv on H was determined by immunoblotting of virions using an anti-measles H antibody. The chimeric H glycoprotein of MV- $\alpha$ FR showed a higher apparent

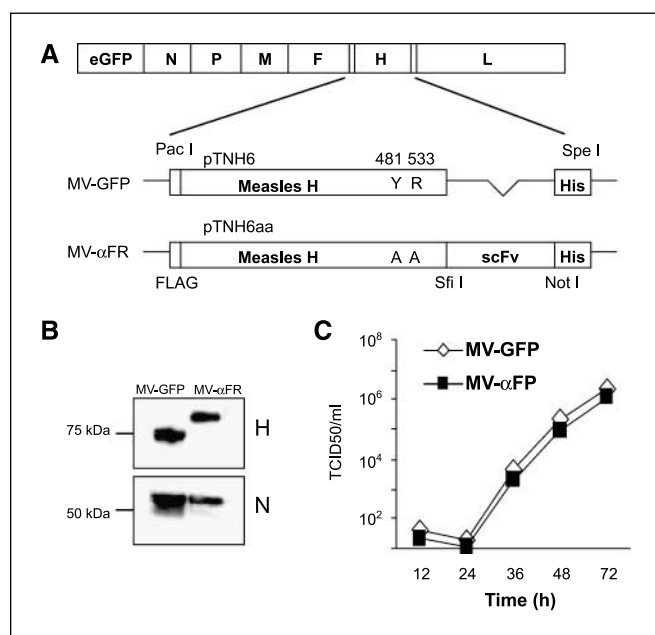


**Fig. 1.** Generation and characterization of the FR $\alpha$ -targeted measles virus. **A**, schematic representation of the unmodified (MV-GFP) and tropism-modified (MV- $\alpha$ FR) measles virus genomes. Mutations in H at 481Y  $\rightarrow$  A and 533R  $\rightarrow$  A ablate CD46/SLAM interaction. A single-chain antibody (scFv) is displayed as a COOH-terminal extension of mutated H protein followed by a six-histidine peptide (H6). **B**, immunoblot of the parental and chimeric virions using anti-H and anti-N antibodies. Equal titers of each virus were loaded. The chimeric H glycoprotein of MV- $\alpha$ FR (lane 2) has a higher molecular weight compared with that of MV-GFP (lane 1). **C**, growth kinetics of MV- $\alpha$ FR and MV-GFP on Vero- $\alpha$ His cells were comparable.

molecular weight than the unmodified H (Fig. 1B). Replication kinetics of MV- $\alpha$ FR was compared with the MV-GFP parental virus in Vero- $\alpha$ His producer cells. The one-step growth curves of both viruses were comparable (Fig. 1C), and viral titer stocks of MV-eGFP and MV- $\alpha$ FR were in the range of  $3 \times 10^7$  and  $1 \times 10^7$  TCID<sub>50</sub>, respectively.

Specificity of MV- $\alpha$ FR infection and cytopathic effects were investigated on a panel of Chinese hamster ovary (CHO) cells expressing the respective receptors, CD46, SLAM, FR $\alpha$ , and CD38. To control for specificity of the  $\alpha$ FR scFv, a recombinant measles virus displaying a scFv against CD38, a plasma cell marker, was used (MV- $\alpha$ CD38). As shown in Fig. 2, CHO cells expressing either CD46 or SLAM were infected by MV-GFP but not by the double-blind fully retargeted MV- $\alpha$ FR or MV- $\alpha$ CD38. FR $\alpha$ -positive CHO cells were infected efficiently by MV- $\alpha$ FR but not by MV- $\alpha$ CD38 that displays an irrelevant scFv and vice versa on CHO-CD38 cells. These data showed that MV- $\alpha$ FR was ablated for infection and cell fusion via both of the native measles virus receptors and is highly specific for FR $\alpha$ . Importantly, the one-step growth kinetics and final titers reached by the fully retargeted virus were not significantly compromised by displayed scFv and compared favorably with the parental virus.

**In vitro tumor-selective killing by FR $\alpha$ -retargeted virus.** Specificity of infection and cell killing by MV- $\alpha$ FR was investigated on a panel of human cancer cell lines and normal cells. The presence or absence of  $\alpha$ FR receptor on these cells was analyzed by flow cytometry (Supplementary Figure). Cells were infected at a multiplicity of infection of 0.5, and after 48 hours, the presence of green fluorescent protein (GFP)-positive syncytia

were noted, and numbers of viable cells were counted by trypan blue exclusion. MV- $\alpha$ FR caused cytopathic damage of extensive cell fusion in ovarian and breast cancer cell lines and not in normal cells and other cancer cell lines (Fig. 3A). In contrast, MV-GFP infected both tumor and normal cells, although the cytopathic damage induced in normal cells was minimal, with significantly fewer and smaller (4-5 nuclei) syncytia (Fig. 3A). These observed cytopathic effects correlated with tumor cell killing as determined by trypan blue exclusion (Fig. 3B). To confirm that infection and cell fusion were mediated specifically via FR $\alpha$ , we used IGROV1-DM99 cells stably transfected with a plasmid encoding a FR $\alpha$ -specific intrabody (MOv19) to knock down FR $\alpha$  expression (27) and also generated A375 cells stably expressing FR $\alpha$  (A375-FR) by lentiviral transduction. As shown in Fig. 3C and D, MV- $\alpha$ FR efficiently infected and caused massive cell fusion in FR $\alpha$ -positive IGROV1 and A375-FR but not in FR $\alpha$ -negative A375 and IGROV1-DM99.

**Specificity of in vivo tumor targeting by MV- $\alpha$ FR.** The *in vivo* targeting specificity of MV- $\alpha$ FR was evaluated in severe combined immunodeficient mice bearing s.c. ARH-77 or ARH-77-FR xenografts. ARH-77 cells express CD46 and SLAM but not FR $\alpha$  or EGFR. MV-GFP and measles viruses retargeted to FR $\alpha$  or EGFR were given i.v. to the mice. Four days after the last injection, tumors were harvested and examined under white light or fluorescence microscopy. As shown in Fig. 4A, both ARH-77 and ARH-77-FR xenografts were infected by the parental untargeted MV-GFP virus. In contrast, MV- $\alpha$ FR infected only the FR $\alpha$ -expressing ARH-77-FR xenografts. MV- $\alpha$ EGFR, which displays a scFv against EGFR, could not infect ARH-77 or ARH-77-FR xenografts.

**Biodistribution of MV- $\alpha$ FR infection in measles-susceptible transgenic mice.** Ifnar-CD46Ge transgenic mice, which express the human CD46 receptor with the same tissue specificity and whose type I IFN receptors were inactivated to facilitate virus spread (29, 30), were used to evaluate the tropism of the MV- $\alpha$ FR virus versus the parental CD46-tropic MV-GFP. Mice were injected i.p. with  $2 \times 10^6$  TCID<sub>50</sub> MV-GFP or MV- $\alpha$ FR, and 48 hours later, mice were euthanized and examined under a fluorescence microscope. Strong GFP signals were observed in the greater omentum and peritoneal linings of mice that received MV-GFP but not MV- $\alpha$ FR (Fig. 4B). GFP-positive cells were also present on mediastinal lymph nodes and spleens of MV-GFP-infected mice (data not shown). These GFP-positive cells were previously shown to be macrophages that concentrate in milky spots on the omentum, peritoneal lining, and marginal zone of the white pulp (30). Thus, the predominant non-target cells that were efficiently infected by MV-GFP are not permissive to infection by the fully retargeted MV- $\alpha$ FR. Other major organs (liver, kidneys, heart, and brain) were negative for GFP expression. However, it is also important to add that delivery of low levels of virus to these normal tissues, not detected using this method, cannot be excluded.

**In vivo antitumor activity of MV- $\alpha$ FR.** We first tested the oncolytic potential of MV- $\alpha$ FR *in vivo* via i.t. administration in a s.c. model of human ovarian cancer using FR $\alpha$ -positive SKOV3ip.1 cells. The FR $\alpha$ -targeted virus induced significant inhibition of tumor growth compared with the saline-treated controls (Fig. 5A). Repeated measures ANOVA showed a statistically significant difference in tumor growth between the MV- $\alpha$ FR-treated and control groups ( $P_{\text{treatment}} < 0.0001$ ,

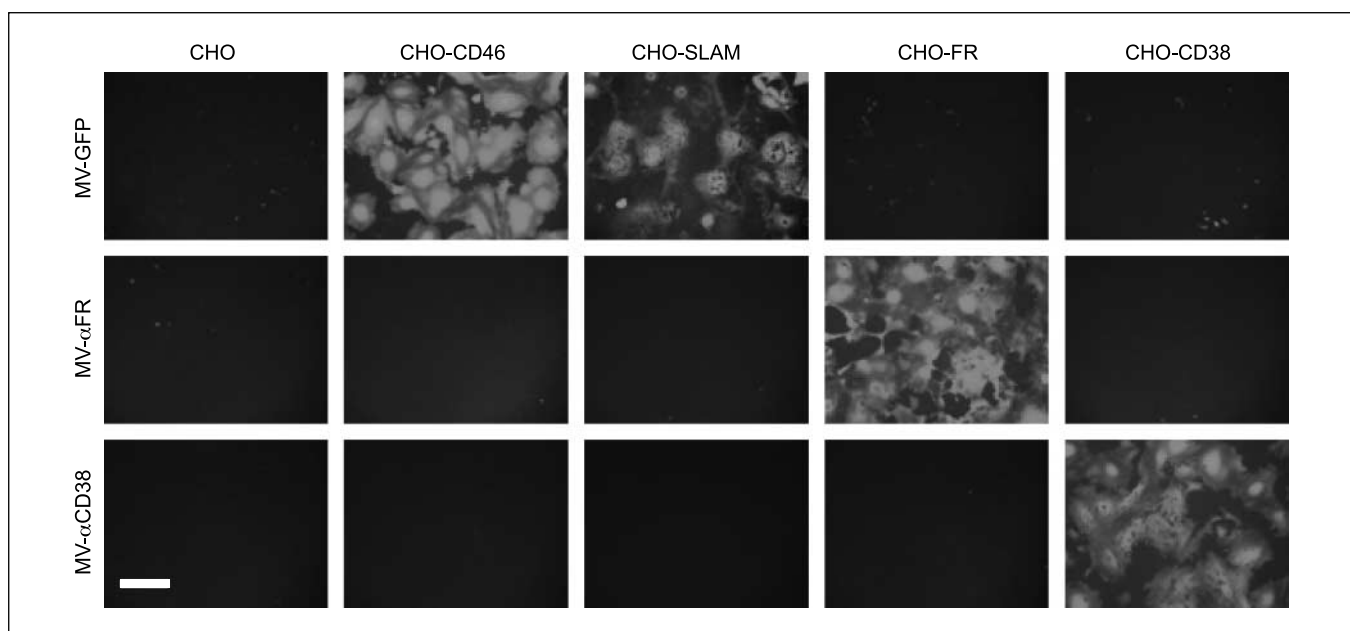


**Fig. 2.** Specificity of FR $\alpha$ -targeted measles virus. The CHO transfectants expressing CD46, SLAM, FR $\alpha$ , and CD38 receptors were infected with respective viruses at a multiplicity of infection of 0.5, and photographs were taken 2 days later. Bar, 0.5 mm.

$P_{\text{time}} < 0.0001$ ,  $P_{\text{interaction}} = 0.034$ ). Therapeutic potency of the  $\alpha$ FR-targeted measles virus was comparable with parental virus killed ovarian cancer cells through CD46 (24). From day 30, some mice in control group had to be euthanized due to tumor burden. In contrast, complete regression of tumors occurred in 5 of 10 and 3 of 10 mice treated with MV- $\alpha$ FR and MV-GFP, respectively.

We next tested the viruses in an i.p. model of disseminated ovarian cancer using SKOV3ip.1 cells stably expressing firefly luciferase and secreted  $\beta$ hCG. I.p. tumor growth was monitored noninvasively using bioluminescence imaging and analysis of plasma  $\beta$ hCG levels. At 4 days after cell implantation, growing i.p. tumors were detected using bioluminescence imaging and found to localize mainly at the greater omentum (Fig. 5B). Mice were treated with the viruses from day 6, every other day for a total of six doses (total dose =  $6 \times 10^6$  TCID<sub>50</sub>). Bioluminescence images revealed that there was significant inhibition of tumor growth in the MV- $\alpha$ FR-treated group compared with the saline control group (Fig. 5B). Differences in tumor burden were quantitated by measuring whole abdominal photon counts and plasma levels of tumor-secreted  $\beta$ hCG (Fig. 5C and D). Two-way repeated measures ANOVA (from day 4 or 6 to day 36) indicated that MV- $\alpha$ FR significantly reduced tumor growth compared with the saline-treated control (photon counts:  $P_{\text{treatment}} = 0.0006$ ,  $P_{\text{time}} = 0.0001$ ,  $P_{\text{interaction}} = 0.0068$  and  $\beta$ hCG:  $P_{\text{treatment}} < 0.0001$ ,  $P_{\text{time}} < 0.0001$ ,  $P_{\text{interaction}} < 0.0001$ ). There was 10-fold less tumor burden in the MV- $\alpha$ FR-treated group compared with control group on day 36 (photon counts:  $P = 0.009$  and  $\beta$ hCG:  $P < 0.0001$ , unpaired *t* test). Survival of mice treated with MV- $\alpha$ FR was superior to that of the control group ( $P < 0.0001$ , log-rank test; Fig. 5E). Five of 10 MV- $\alpha$ FR-treated mice and 3 of 10 MV-GFP-treated mice were alive at the end of the experiment (day 90). All of these mice were euthanized, and gross examination of mice

revealed no residual i.p. tumors, although some of them still had a s.c. injection site tumor.

## Discussion

Here, we have generated an oncolytic measles virus with tight specificity for FR $\alpha$  receptor and have shown the virus to be therapeutically active in human ovarian cancer xenograft models. FR $\alpha$  is a very attractive cancer target. It is expressed in 70% and 40%, respectively, of ovarian and breast cancer cases seen in our cancer clinic (Supplementary Fig. S1B).<sup>6</sup> In contrast, its expression on normal tissues is restricted to apical surfaces of polarized epithelial where it has limited contact with circulating cytotoxic drugs (14, 15, 17). This study adds a new class of anticancer agent, an oncolytic virus, to the repertoire of FR-targeted experimental therapeutics (31) that already include monoclonal antibodies (21, 32, 33), bispecific antibody-targeted T cells (22, 23, 34, 35), and DNA vaccines (36). Because the cytotoxic agent typically reaches only a small percentage of cells in the tumor, live viruses are very attractive as anticancer agents as they can replicate and potentially spread from the initial infected cell to surrounding cell layers. An additional dimension to measles virotherapy is its mechanism of tumor cell killing through induction of extensive intercellular fusion between the infected cell and neighboring uninfected cells and significantly increasing the bystander killing index of this agent (8, 24).

Use of replication-competent viruses for cytoreductive cancer therapy (virotherapy) is not new. Various human and animal RNA viruses have been injected into cancer patients in the 1950s to 1970s, and results have both been intriguing and promising (37). Tumor selectivity is typically conferred by

<sup>6</sup> L.C. Hartmann, unpublished data.

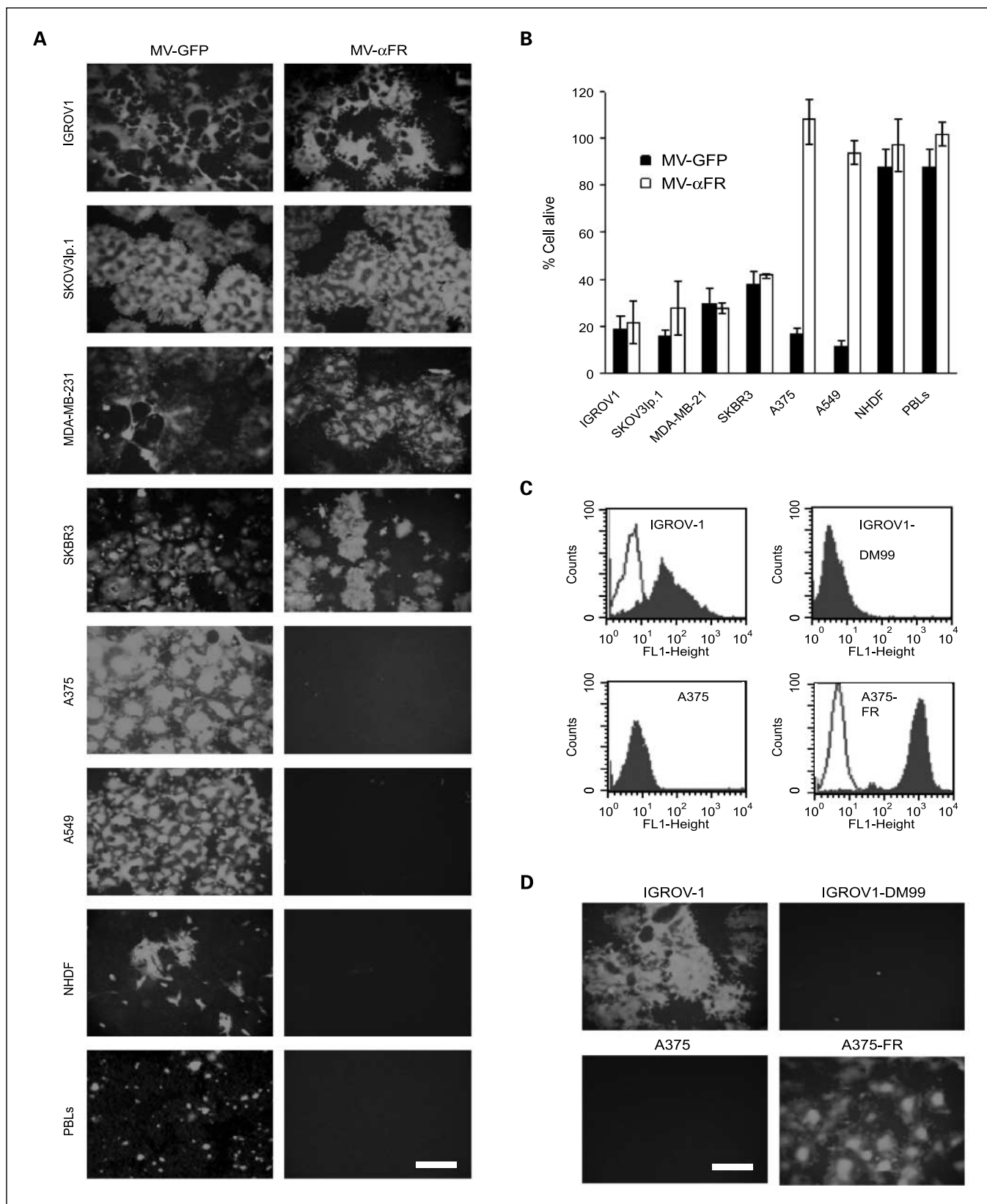


**Fig. 3.** *In vitro* tumor selective killing by FR $\alpha$ -targeted measles virus. Human tumor cell lines and normal cells were infected with the respective viruses at a multiplicity of infection of 0.5. *A*, photographed 2 days after infection. *B*, numbers of viable cells were counted by trypan blue exclusion at 3 days after infection. Columns, means from three replicates; bars, SD. Solid columns, MV-GFP; open columns, MV- $\alpha$ FR. *C*, flow cytometry data on FR expression (filled histogram) in IGROV-1 and A375-FR, IGROV-DM99, and A375 compared with isotype control (empty histogram). *D*, cells were infected with MV- $\alpha$ FR (multiplicity of infection = 0.5) and photographed 2 days after infection. Bar, 0.5 and 0.2 mm for peripheral blood lymphocytes.

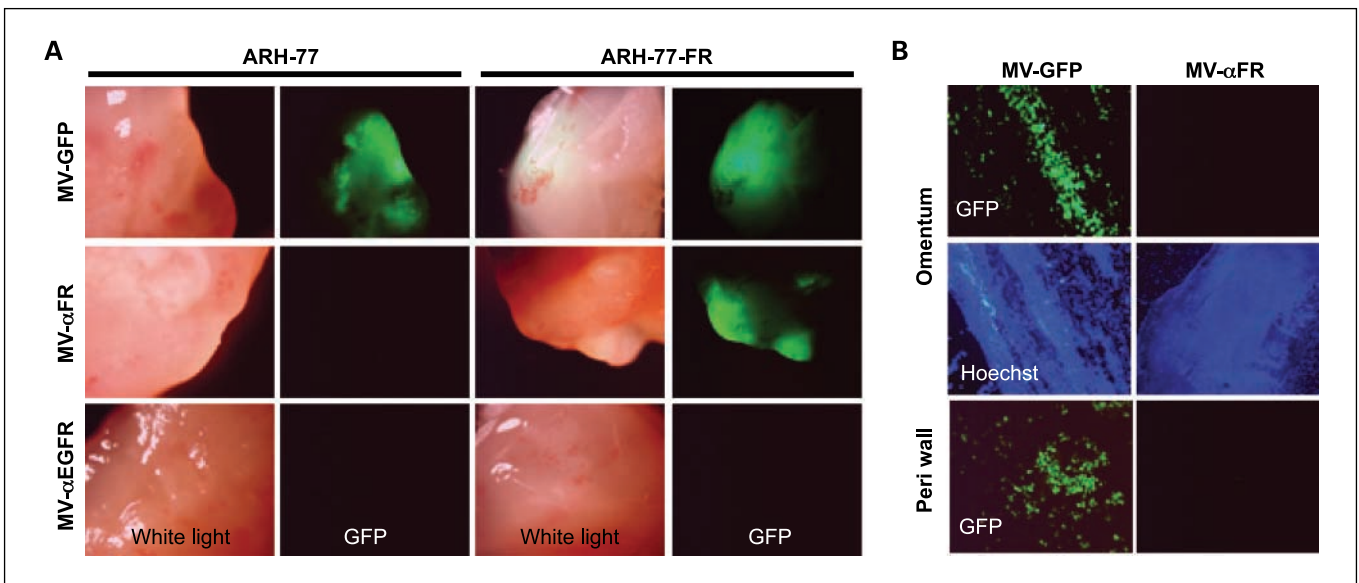


**Fig. 4.** *In vivo* specificity of MV- $\alpha$ FR. **A**, severe combined immunodeficient mice bearing s.c. ARH-77 or ARH-77-FR xenografts were injected twice i.v. via the tail vein ( $n = 3$  per group) with  $2 \times 10^6$  TCID<sub>50</sub> viruses. Tumors were harvested 4 days later and examined under white light or blue light (GFP fluorescence). Photographs of representative tumors. **B**, omentum and peritoneal linings from Ifnar-CD46Ge transgenic mice that received  $2 \times 10^6$  TCID<sub>50</sub> MV-GFP or MV- $\alpha$ FR i.p. Tissues were harvested 2 days later, stained with Hoechst 33342, and examined under blue light for GFP fluorescence.

innate cellular antiviral defenses that protect normal tissues from unwanted damage. These protective mechanisms are in general defective in tumor cells, making them permissive to viral infections (38). Recent progresses in molecular engineering and virus rescue systems have enabled us to control tumor selectivity in new generations of “designer” tumor-selective viruses; these strategies either target defects in the intracellular genetic pathways or receptor usage (39, 40). Here, we have ablated the native tropisms of measles virus and redirected virus attachment, entry, and cytopathic effects to the tumor antigen via a scFv. Because measles is a negative-strand RNA virus with an estimated genomic mutation rate of 1.43 per replication (41), there is a possibility that the mutations introduced into the H protein are not stable, and reversion mutants that regain CD46 or SLAM usage might arise after serial passages of the virus in culture. Efforts have been made to minimize that possibility during the design of those mutations (42), and these fully retargeted measles viruses have been remarkably stable in their receptor usage after multiple serial passages in receptor-positive and receptor-negative cells (12, 43).

Accessibility of the tumor antigen to virus in the circulation is paramount to ensure efficient virus delivery to and infection of the tumor cells. Because ovarian cancer is localized mainly in the peritoneal cavity, i.p. administration of the virus puts it into direct contact with the cancer cells, bypassing the need for vascular delivery. We also showed here that after systemic administration into tumor-bearing mice, the MV- $\alpha$ FR virus was able to attach to and infect FR-positive tumor xenografts. Its access to the tumor antigens was probably facilitated by the leaky tumor vasculature (44). A strategy to improve vector localization is to target the virus to antigens on tumor neovessels (45). Identification of unique antigens on tumor neovessels, the availability of ligands for these targets, and the robustness of the vector retargeting technology are pertinent to the success of this endeavor. The measles retargeting technology is highly flexible; it can accommodate additional large polypeptides, such as

scFvs, to mediate efficient virus entry and achieve titers that are comparable with that of the parental unmodified virus. Clearly, not all ligands displayed on measles virus will be functional, but this technology is a significant improvement compared with retroviral display (46). In fact, the scFv used in this study was first generated and displayed on the murine leukemia retrovirus. Vector attachment to FR $\alpha$  was redirected, but gene delivery was not achieved (47). Display of scFvs on adenoviruses remains challenging as the folding of scFv occurs in the endoplasmic reticulum, whereas adenoviral assembly does not (48, 49).

Interaction of wild-type measles virus with SLAM causes a profound but transient immunosuppression in infected individuals (11, 50, 51). Attenuated measles viruses, although less immunosuppressive, also use CD46 that is ubiquitously expressed at low levels on all nucleated cells. We hypothesize that ablation of CD46 and SLAM interactions should enhance the safety profiles, especially at the higher dose levels used in cancer therapy, of these fully retargeted viruses. Our preliminary studies using mixed lymphocyte reaction assays indicated that these fully retargeted viruses with ablated tropisms for CD46/SLAM do not inhibit lymphocyte proliferation.<sup>7</sup> In this study, we have also attempted to address potential decrease in toxicity by using measles susceptible genetically modified mice that express human CD46 with the same tissue specificity (29). Macrophages that were the predominant cell type infected by the parental virus were not infected by MV- $\alpha$ FR. Ablation of CD46 tropism could also minimize vector wastage to non-target cells, potentially enhance virus availability to the tumor cells, and achieve a more favorable therapeutic outcome. Because these transgenic mice do not also express the human FR $\alpha$ , it is difficult to evaluate potential toxicity of the virus and will require testing in non-human primates before initiation of a clinical study. In addition,

<sup>7</sup> T. Nakamura, unpublished data.

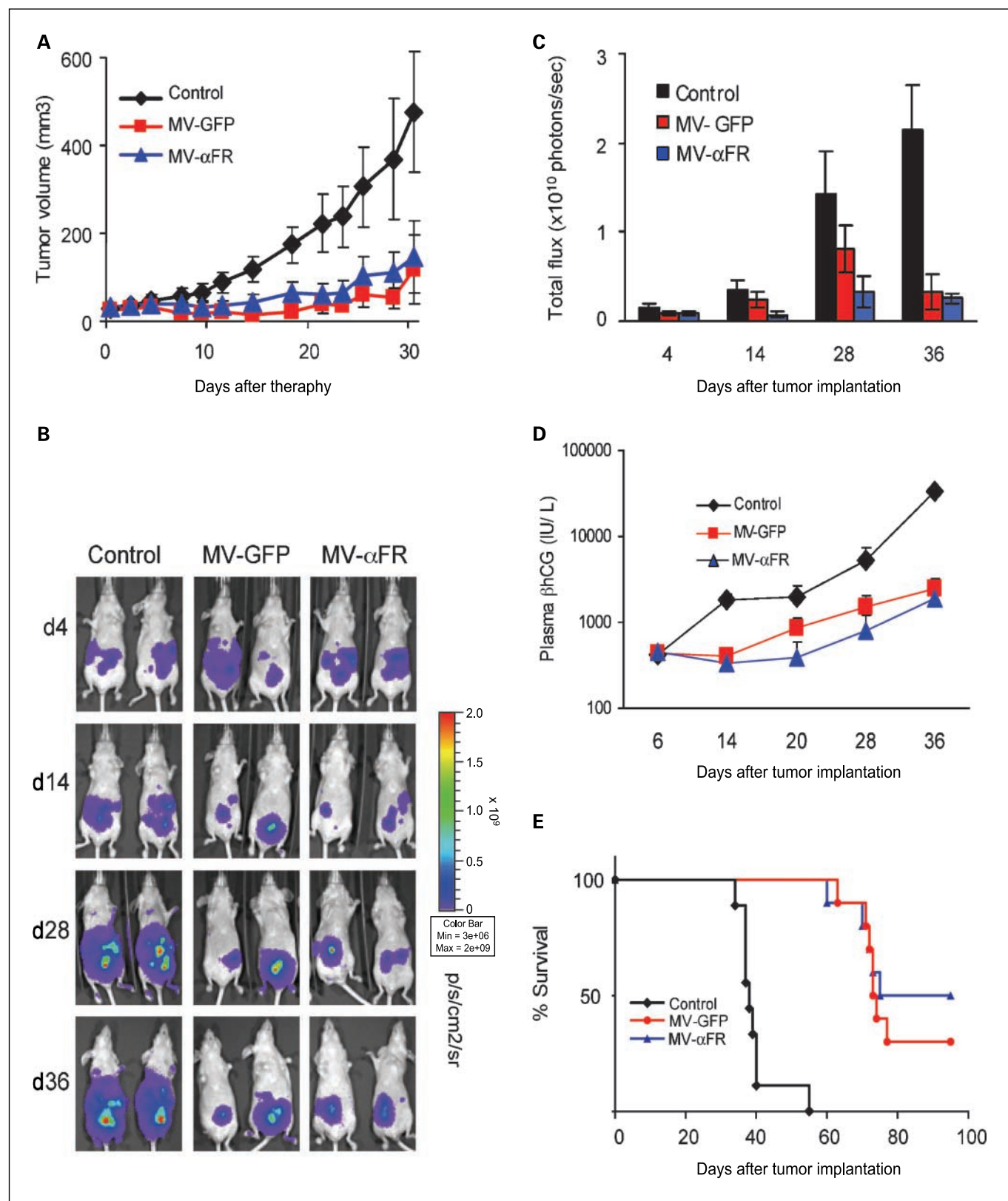


**Fig. 5.** *In vivo* antitumor activity of MV-αFR. **A**, tumor growth curves of s.c. SKOV3ip.1 xenografts treated by i.t. virus administration. Mice received a total of four doses of each virus at  $5 \times 10^5$  TCID<sub>50</sub> per dose ( $n = 10$  mice per virus treated group) or saline (control,  $n = 9$ ). Tumor volumes were calculated using the formula:  $0.5 \times \text{length} \times \text{width}^2$ . **B** to **E**, i.p. model of ovarian cancer. SKOV3ip.1-Fluc-βhCG cells were injected i.p., and 6 days later, mice received a total of six doses of  $1 \times 10^6$  TCID<sub>50</sub> of MV-GFP or MV-αFR i.p. ( $n = 9$  for saline control and  $n = 10$  for treatment groups). **B**, representative images of mice from bioluminescent imaging. Quantitation of tumor burden from (C) bioluminescent imaging or by (D) measuring plasma βhCG levels. Photon counts were calculated from the imaging data using the IVIS Living Image software. **E**, Kaplan-Meier survival curves of mice in the i.p. model. Points, means; bars, SE.

the true toxicity profiles of these retargeted viruses would be revealed in a careful dose escalation clinical trial.

Clearly, one of the major issues with use of measles virotherapy is the presence of preexisting neutralizing antibodies that could inhibit virus infectivity. Currently, we have no good methods to deplete these neutralizing antibodies, although it is an area under active investigation in our laboratories. Because ovarian cancer cells are localized mainly in the peritoneal cavity, intracavity administration of the virus is a feasible option to bypass antibodies in the circulation. This is the basis for the current trial to use i.p. instead of intravascular delivery. Virus inactivation is a balance between neutralization kinetics and virus numbers; it might be possible for some of the input virus to reach the target site before all viruses are neutralized. Indeed, sera with low titers of anti-measles antibodies are less effective at neutralizing a given titer of input virus.<sup>8</sup>

<sup>8</sup> K.-W. Peng, unpublished data.

## References

- Nakamura T, Russell SJ. Oncolytic measles viruses for cancer therapy. *Expert Opin Biol Ther* 2004;4:1685–92.
- Heinzerling L, Kunzi V, Oberholzer PA, Kundig T, Naim H, Dummer R. Oncolytic measles virus in cutaneous T-cell lymphomas mounts antitumor immune responses *in vivo* and targets interferon-resistant tumor cells. *Blood* 2005;106:2287–94.
- Peng KW, Facteau S, Wegman T, O’Kane D, Russell SJ. Non-invasive *in vivo* monitoring of trackable viruses expressing soluble marker peptides. *Nat Med* 2002;8:527–31.
- Dingli D, Peng KW, Harvey ME, et al. Image-guided radiovirotherapy for multiple myeloma using a recombinant measles virus expressing the thyroidal sodium iodide symporter. *Blood* 2004;103:1641–6.
- Phuong LK, Allen C, Peng KW, et al. Use of a vaccine strain of measles virus genetically engineered to produce carcinoembryonic antigen as a novel therapeutic agent against glioblastoma multiforme. *Cancer Res* 2003;63:2462–9.
- Dorig RE, Marcil A, Chopra A, Richardson CD. The human CD46 molecule is a receptor for measles virus (Edmonston strain). *Cell* 1993;75:295–305.
- Tatsuo H, Ono N, Tanaka K, Yanagi Y. SLAM (CDw150) is a cellular receptor for measles virus. *Nature* 2000;406:893–7.
- Galanis E, Bateman A, Johnson K, et al. Use of viral fusogenic membrane glycoproteins as novel therapeutic transgenes in gliomas. *Hum Gene Ther* 2001;12:811–21.
- Riley-Vargas RC, Gill DB, Kemper C, Liszewski MK, Atkinson JP. CD46: expanding beyond complement regulation. *Trends Immunol* 2004;25:496–503.
- Schneider-Schaules S, Schneider-Schaules J, Niewiesk S, Ter Meulen V. Measles virus: immunomodulation and cell tropism as pathogenicity determinants. *Med Microbiol Immunol (Berl)* 2002;191:83–7.
- Hahm B, Arbour N, Nanche D, Homann D, Manchester M, Oldstone MB. Measles virus infects and suppresses proliferation of T lymphocytes from transgenic mice bearing human signaling lymphocytic activation molecule. *J Virol* 2003;77:3505–15.
- Nakamura T, Peng KW, Harvey M, et al. Rescue and propagation of fully retargeted oncolytic measles viruses. *Nat Biotechnol* 2005;23:209–14.
- Jemal A, Murray T, Ward E, et al. Cancer statistics, 2005. *CA Cancer J Clin* 2005;55:10–30.
- Lu Y, Low PS. Immunotherapy of folate receptor-expressing tumors: review of recent advances and future prospects. *J Control Release* 2003;91:17–29.
- Elnakat H, Ratnam M. Distribution, functionality and gene regulation of folate receptor isoforms: implications in targeted therapy. *Adv Drug Deliv Rev* 2004;56:1067–84.
- Wu M, Gunning W, Ratnam M. Expression of folate receptor type  $\alpha$  in relation to cell type, malignancy, and differentiation in ovary, uterus, and cervix. *Cancer Epidemiol Biomarkers Prev* 1999;8:775–82.
- Weitman SD, Lark RH, Coney LR, et al. Distribution of the folate receptor GP38 in normal and malignant cell lines and tissues. *Cancer Res* 1992;52:3396–401.
- Bueno R, Appasani K, Mercer H, Lester S, Sugarbaker D. The  $\alpha$  folate receptor is highly activated in malignant pleural mesothelioma. *J Thorac Cardiovasc Surg* 2001;121:225–33.
- Toffoli G, Cernigoi C, Russo A, Gallo A, Bagnoli M, Boiocchi M. Overexpression of folate binding protein in ovarian cancers. *Int J Cancer* 1997;74:193–8.
- Zhao XB, Lee RJ. Tumor-selective targeted delivery of genes and antisense oligodeoxyribonucleotides via the folate receptor. *Adv Drug Deliv Rev* 2004;56:1193–204.
- van Zanten-Przybysz I, Molthoff CF, Roos JC, et al. Radioimmunotherapy with intravenously administered <sup>131</sup>I-labeled chimeric monoclonal antibody MOv18 in patients with ovarian cancer. *J Nucl Med* 2000;41:1168–76.
- Canevari S, Stoter G, Arienti F, et al. Regression of advanced ovarian carcinoma by intraperitoneal treatment with autologous T lymphocytes retargeted by a bispecific monoclonal antibody. *J Natl Cancer Inst* 1995;87:1463–9.
- Miotti S, Negri DR, Valota O, et al. Level of anti-mouse-antibody response induced by bi-specific monoclonal antibody OC/TR in ovarian-carcinoma patients is associated with longer survival. *Int J Cancer* 1999;84:62–8.
- Peng KW, TenEyck CJ, Galanis E, Kalli KR, Hartmann LC, Russell SJ. Intraperitoneal therapy of ovarian cancer using an engineered measles virus. *Cancer Res* 2002;62:4656–62.
- Peng KW, Donovan KA, Schneider U, Cattaneo R, Lust JA, Russell SJ. Oncolytic measles viruses displaying a single-chain antibody against CD38, a myeloma cell marker. *Blood* 2003;101:2557–62.
- Anderson BD, Nakamura T, Russell SJ, Peng KW. High CD46 receptor density determines preferential killing of tumor cells by oncolytic measles virus. *Cancer Res* 2004;64:4919–26.
- Figini M, Ferri R, Mezzanzanica D, et al. Reversion of transformed phenotype in ovarian cancer cells by intracellular expression of anti folate receptor antibodies. *Gene Ther* 2003;10:1018–25.
- Hasegawa K, Pham L, O’Connor MK, Federspiel MJ, Russell SJ, Peng KW. Dual therapy of ovarian cancer using measles viruses expressing carcinoembryonic antigen and sodium iodide symporter. *Clin Cancer Res* 2006;12:1868–75.
- Mrkic B, Pavlovic J, Rulicke T, et al. Measles virus spread and pathogenesis in genetically modified mice. *J Virol* 1998;72:7420–7.
- Peng KW, Frenze M, Myers R, et al. Biodistribution of oncolytic measles virus after intraperitoneal administration into Ifnar-CD46G transgenic mice. *Hum Gene Ther* 2003;14:1565–77.
- Hilgenbrink AR, Low PS. Folate receptor-mediated drug targeting: from therapeutics to diagnostics. *J Pharm Sci* 2005;94:2135–46.
- Coney LR, Mezzanzanica D, Sanborn D, Casalini P, Colnaghi MI, Zurawski VR, Jr. Chimeric murine-human antibodies directed against folate binding receptor are efficient mediators of ovarian carcinoma cell killing. *Cancer Res* 1994;54:2448–55.
- Crippa F, Bolis G, Seregini E, et al. Single-dose intraperitoneal radioimmunotherapy with the murine monoclonal antibody I-131 MOv18: clinical results in patients with minimal residual disease of ovarian cancer. *Eur J Cancer* 1995;31A:686–90.
- Mazzoni A, Mezzanzanica D, Jung G, Wolf H, Colnaghi MI, Canevari S. CD3-CD28 costimulation as a means to avoiding T cell preactivation in bispecific monoclonal antibody-based treatment of ovarian carcinoma. *Cancer Res* 1996;56:5443–9.
- Kershaw MH, Westwood JA, Hwu P. Dual-specific T cells combine proliferation and antitumor activity. *Nat Biotechnol* 2002;20:1221–7.
- Neglia F, Orengo AM, Cilli M, et al. DNA vaccination against the ovarian carcinoma-associated antigen folate receptor  $\alpha$  (FR $\alpha$ ) induces cytotoxic T lymphocyte and antibody responses in mice. *Cancer Gene Ther* 1999;6:349–57.
- Russell SJ. RNA viruses as virotherapy agents. *Cancer Gene Ther* 2002;9:961–6.
- Parato KA, Senger D, Forsyth PA, Bell JC. Recent progress in the battle between oncolytic viruses and tumours. *Nat Rev Cancer* 2005;5:965–76.
- Campbell SA, Gromeier M. Oncolytic viruses for cancer therapy II. Cell-internal factors for conditional growth in neoplastic cells. *Onkologie* 2005;28:209–15.
- Campbell SA, Gromeier M. Oncolytic viruses for cancer therapy I. Cell-external factors: virus entry and receptor interaction. *Onkologie* 2005;28:144–9.
- Schrag SJ, Rota PA, Bellini WJ. Spontaneous mutation rate of measles virus: direct estimation based on



- mutations conferring monoclonal antibody resistance. *J Virol* 1999;73:51–4.
42. Nakamura T, Peng KW, Vongpunsawad S, et al. Antibody-targeted cell fusion. *Nat Biotechnol* 2004; 22:331–6.
43. Hadac EM, Peng KW, Nakamura T, Russell SJ. Reengineering paramyxovirus tropism. *Virology* 2004; 329:217–25.
44. Hashizume H, Baluk P, Morikawa S, et al. Openings between defective endothelial cells explain tumor vessel leakiness. *Am J Pathol* 2000;156:1363–80.
45. Liu Y, Deisseroth A. Tumor vascular targeting therapy with viral vectors. *Blood* 2006;107:3027–33.
46. Lavillette D, Russell SJ, Cosset FL. Retargeting gene delivery using surface-engineered retroviral vector particles. *Curr Opin Biotechnol* 2001;12:461–6.
47. Pizzato M, Blair ED, Fling M, et al. Evidence for nonspecific adsorption of targeted retrovirus vector particles to cells. *Gene Ther* 2001;8: 1088–96.
48. Mizuguchi H, Hayakawa T. Targeted adenovirus vectors. *Hum Gene Ther* 2004;15:1034–44.
49. Hedley SJ, Auf der Maur A, Hohn S, et al. An adenovirus vector with a chimeric fiber incorporating stabilized single chain antibody achieves targeted gene delivery. *Gene Ther* 2006;13:88–94.
50. Slifka MK, Homann D, Tishon A, Pagarigan R, Oldstone MB. Measles virus infection results in suppression of both innate and adaptive immune responses to secondary bacterial infection. *J Clin Invest* 2003;111:805–10.
51. Schneider-Schaulies S, Niewiesk S, Schneider-Schaulies J, ter Meulen V. Measles virus induced immunosuppression: targets and effector mechanisms. *Curr Mol Med* 2001;1:163–81.
52. Leamon CP, Low PS. Folate-mediated targeting: from diagnostics to drug and gene delivery. *Drug Discov Today* 2001;6:44–51.
53. Reddy JA, Xu LC, Parker N, Vetzal M, Leamon CP. Preclinical evaluation of (99 m)Tc-EC20 for imaging folate receptor-positive tumors. *J Nucl Med* 2004;45: 857–66.